Evaporation of Hydrocarbon Fuel Droplet under Elevated Temperatures

Dr. Abdulhassan Abid Karamallah*
& Muna Khalil Asmail

Received on: 13/12/2009
Accepted on:6/5/2010

Abstract

Extended model is a theoretical and analytical model for evaporation of hydrocarbon fuel droplet. This model assumes that there is a moving hydrocarbon fuel droplet in quasisteady environmental air. Four types of fuel (n-heptane, n-hexane, n-decan, and light Diesel) are used for analysis at atmospheric pressure and temperatures from about (300 – 1500) K. The initial droplet size used is 100 µm for a Reynolds number ranging from (0.1– 1800). Computer programs have been developed in (Matlab-7) language to find out the mass evaporation rate, variation of size, droplet life time, and flame stand off ratio. The percentage value for maximum mass evaporation rate from the extended model is (0.13%) greater than that obtained from the mass evaporation rate from classical model due to the increasing of the heat gain to the movement drop. the results are compared with the existing theoretical and experimental work in literature and acceptable agreements are obtained

تبخر قطرة الوقود الهايدروكاربوني تحت درجات حرارة عالية

الخلاصة

النموذج الموسع هو نموذج رياضي وتحليلي لغرض دراسة تبخر قطرات الوقود السائل وذلك على افتراض أن القطرة تتحرك ضمن جو من الهواء الشبه ساكن. وقد تمت الدراسة لأربعة من أنواع الوقود وهي (الهبتان الهكسان الديكان والديزل الخفيف) تحت ضغط جوي طبيعي ودرجات حرارة محيطية تراوحت (300-1500) وبقطر ابتدائي 100 مايكرو متر للقطرة ولإعداد رينولد تراوحت من (0.1-1800) . تم أعداد برامج حاسوب بلغة (Matlab-7) لإيجاد معدل الكتلة المتبخرة,التغيير بالحجم وحساب عمر القطرة و نسبة موقع اللهب ودرجة حرارة اللهب. وقد وجد إن نسبة المئوية لمعدل الكتلة المتبخرة من تطبيق الموديل الموسع هي (0.13%) أكثر مما في حالة استخدام الموديل التقليدي بسبب الزيادة في الحرارة المكتسبة الى القطرة المتحركة. تم مقارنة النتائج مع الاعمال النظرية والعملية المتوفرة في المراجع ووجد ان هناك تطابقا مقبولا

Introduction

For modern combustion engines using liquid fuels, several processes play important roles in reaching high efficiency in the combustion cycle and low emissions in the exhaust gas. One of these processes is the evaporation of the fuel in the combustion chamber. For direct injection systems used in aircraft or car engines, the fuel enters the combustion chamber in the liquid state. During injection, the liquid disintegrates into single droplets by atomization. In addition, the droplets evaporate before combustion occurs, figure (1) shows the state of droplet evaporation [1].The theory of fuel droplet vaporization has been intensively developed during the past several decades. The classical droplet vaporization mode1 explained in many literature [2,3], deals with an isolated pure component single droplet suddenly exposed to a hot environment at low pressure. Since

*Mechanical Engineering Department, University of Technology /Baghdad
**Center of Training & Workshops, University of Technology /Baghdad

https://doi.org/10.30684/etj.28.17.2
2412-0758/University of Technology-Iraq, Baghdad, Iraq

the droplet temperature is lower than the surrounding atmosphere temperature, a net driving force due to temperature difference will transfer heat into the droplet, which will be used to supply energy for vaporization as well as for heating the liquid. As the droplet heats up, the vapour concentration will start to build up at the liquid-vapour interface where equilibrium between the liquid and vapour exists; this will be a function of interface temperature and the total atmospheric pressure. The vapour will start to diffuse into the surrounding air, resulting a net mass flux outward from the droplet. Sirignano and Law [4], studied the effect of non-uniform liquid-phase temperatures on a single component fuel droplet by considering that internal motion does not exist and diffusion is the only heat transport mechanism. They compared this case with that of a uniform liquid-phase temperature (complete mixing model) and they concluded that the droplet size variations and consequently the droplet vaporization time can be predicted with good accuracy regardless of the mode1 of internal heat transfer. Law [5], presented a review for the progresses on understanding the fundamental mechanisms governing droplet vaporization and combustion. Topics include the d2-law and its limitations; the major transient processes of droplet heating and fuel vapor accumulation; effects due to variable transport property assumptions; combustion of multi-component fuels including the miscible fuel blends, immiscible emulsions, and coal-oil mixtures, finite-rate kinetics leading to ignition and extinction; and droplet interactions, have been presented.

2 Extension to convective environment model:

The purpose of this model is to study the effect of the convective transport caused by the relative velocity between the droplet and the free stream on the evaporation process of a single component droplet suddenly exposed to a hot environment.

The essence of film theory is the replacement of the heat and mass transfer boundary conditions at infinity with the same conditions moved in ward to the so-called film radius, d_M for species, and d_T for energy [6].

The film radii are defined in terms of the Nusselt number Nu, for heat transfer, and the Sherwood number Sh, for mass transfer, given by,

$$\frac{d_T}{r_S} = \frac{Nu}{Nu-2} \quad (1)$$

$$\frac{d_M}{r_S} = \frac{Sh}{Sh-2} \quad (2)$$

For a stagnant medium $Nu = 2$; thus, recover $d_T \to \infty$ in the absence of convection. Consistent with the unity Lewis number assumption, assume $Sh = Nu$. For droplet burning with forced convection, at low Reynolds number limit [7]:

(Nu or Sh)=2+1/2(Re.Pr or Re.Sc) +higher order terms (3)

Other studies of evaporation in creeping motion show that the coefficient, 1/2, depends on the variable properties model and degree of overall properties variation in the flow field around the drop, and neglecting the higher order terms in Eqn. (3) yields a prediction that is within 2% of the more complete expansion.

At the higher Reynolds number, the Ranz and Marshall correlation given in this Eqn. from [8]:

$$Nu = 2 + 0.6\,\mathrm{Re}^{1/2}\,\mathrm{Pr}^{1/3} \quad (4)$$

Employing the frössling correlation for forced convection, we have,

$$Nu = 2 + 0.555\,\mathrm{Re}^{1/2}\,\mathrm{Pr}^{1/3} \quad (5)$$

For (10<Re<1800)

At the higher Reynolds numbers, Yuge suggests a higher power for the Reynolds number, in agreement with other measurement. Combining Eqn. (3) and (5) to obtain a synthesized correlation which approaches the correct limiting values at low and high Reynolds numbers (Re<1800)

$$Nu = 2 + \left[0.555\,\mathrm{Re}^{\frac{1}{2}}\,\mathrm{Pr}^{\frac{1}{3}} \Big/ \left(1 + 1.232 \Big/ \left(\mathrm{Re}(\mathrm{Pr})^{\frac{4}{3}} \right) \right)^{\frac{1}{2}} \right] \quad (6)$$

Where:

$$\mathrm{Re}_d = \frac{2 r_s \left| v_d - v_g \right|}{u_g} \quad (7)$$

$$\mathrm{Pr}_d = \frac{Cp_g \mu_g}{l_g} \quad (8)$$

v_d And v_g are droplet and gas velocities, u_g and μ_g are gas kinematics and dynamic viscosities, Cp and l_g are gas specific heat capacity at constant pressure and thermal conductivity, respectively. (See Figure (2)).

The major assumptions used for the extension to convective environment model are,

1- The burning droplet surrounded by a spherically symmetric flame, exists in a quiescent and infinite medium. There are no interactions with any other droplets.

2- burning process is quasi-steady.

3- The fuel is a single-component liquid with zero solubility for gases. Phase equilibrium prevails at the liquid-vapor interface.

4- The pressure is uniform and constant.

5- Fuel and oxidizer react in stoichiometric proportions at the flame.

Chemical kinetics are assumed to be infinitely fast, resulting in the flame being represented as an infinitesimally thin sheet.

6- Constant and uniform temperature (initial transient of droplet temperature is neglected).

7- The Lewis number $Le = a/D = l_g / \rho Cp_g D$ is unity.

8- Radiation heat transfer is negligible.

9- The gas-phase thermal conductivity, l_g specific heat, Cp_g, and the product of the density and mall diffusivity, ρD, are all constants.

10- The effect of the convective transport caused by the droplet motion relative to the gas is accounted

2.1 Conservation of mass:-

With the assumption of quasi-steady burning. The mass flow rate $\dot{m}(r)$ is a constant, independent of radius, thus [6],

$$\dot{m} = \dot{m}_F = \rho v_r 4\pi r^2 = \text{constant.} \quad (9)$$

Where

v_r is the Radial velocity

2.2 Species conservation:

For the outer region bounded by ($r_f \le r \le d_M$), the boundary

conditions for species conservation are:

$$d_M = \frac{r_s Nu}{Nu-2} \quad (10)$$

$$Y_{ox}(d_M) = 1 \quad (11)$$

the general solution of oxidizer distribution is,

$$Y_{ox}(r) = u\left\{\frac{\exp\left[-\frac{\dot{m}_f}{4\pi r Dr}\right]}{\exp\left[-\frac{\dot{m}_f}{4\pi r Dr_f}\right]} - 1\right\}$$

For outer region:

$$\frac{\exp\left[-\frac{\dot{m}_F}{4\pi r Dr_s Nu/(Nu-2)}\right]}{\exp\left[-\frac{\dot{m}_F}{4\pi r Dr_f}\right]} = \frac{u+1}{u} \quad (12)$$

2.3 Energy conservation:-

For spherical droplet and axisymmetric geometries, the Shvab-Zeldovich energy equation is given in the form [9],

$$\frac{1}{r^2}\frac{d}{dr}\left\{r^2\left(\rho v_r \int Cp_g dT - \rho D\frac{d\int Cp_g dT}{dr}\right)\right\} = -\sum h_{f,i}^0 \dot{w}_i''' \quad (13)$$

With the assumptions of constant properties, unity Lewis number, zero reaction rate and pure evaporation equation (13), after arrangement can be written as,

$$\frac{d\left(r^2\frac{dT}{dr}\right)}{dr} = \frac{\dot{m}_F Cp_g}{4\pi\lambda_g}\frac{dT}{dr} \quad (14)$$

For the outer region bounded by $(r_f \le r \le d_T)$, the temperature distribution is obtained from the application of the boundary conditions:-

$$T(r_f) = T_f \quad (15)$$

$$T(d_T) = T_\infty \quad (16)$$

The equation of the temperature distribution for general solution at the gas-phase of the burning droplet is:

$$T(r) = \frac{C_1 \exp\left[-\frac{\dot{m}_f Cp_g}{4\pi\lambda_g r}\right]}{\frac{\dot{m}_F Cp_g}{4\pi\lambda_g}} + C_2$$

Where, C_1 and C_2, the constants of integration.

For convenience, if

$$Z_T = \frac{Cp_g}{4\pi\lambda_g} \quad (17)$$

Then, the temperature distribution equation becomes:-

$$T(r) = \frac{C_1 \exp\left[-\frac{Z_T \dot{m}_F}{r}\right]}{Z_T \dot{m}_F} + C_2 \quad (18)$$

Applying the boundary condition, Eqn (15), in Eqn. (18) to obtain:-

$$T_f = \frac{C_1 \exp\left[-\frac{Z_T \dot{m}_F}{r_f}\right]}{Z_T \dot{m}_F} + C_2 \quad (19)$$

Then, the temperature distribution becomes:-

$$T(r) = \frac{C_1\left\{\exp\left[-\frac{Z_T \dot{m}_F}{r}\right] - \exp\left[-\frac{Z_T \dot{m}_F}{r_f}\right]\right\} + T_f Z_T \dot{m}_F}{Z_T \dot{m}_F} \quad (20)$$

Again applying the boundary condition, Eqn (16), into Eqn. (20) yields,

$$T_{\infty}=\frac{C_1\left\{\exp\left[-\frac{Z_T\dot{m}_F(Nu-2)}{r_s Nu}\right]-\exp\left[-\frac{Z_T\dot{m}_F}{r_f}\right]\right\}+T_f Z_T\dot{m}_F}{Z_T\dot{m}_F} \quad (21)$$

Finally, the temperature distribution can be found by substituting these expressions for C_1 and C_2 ,respectively, back into the general solution given by Eqn. (18), result,

$$T(r)=\frac{\left\{(T_{\infty}-T_f)\exp\left(\frac{-Z_T\dot{m}_F}{r}\right)-T_{\infty}\exp\left[\frac{-Z_T\dot{m}_F}{r_f}\right]+T_f\exp\left[\frac{-Z_T\dot{m}_F(Nu-2)}{r_s Nu}\right]\right\}}{\exp\left[\frac{-Z_T\dot{m}_F}{r_f}\right]-\exp\left[\frac{-Z_T\dot{m}_F(Nu-2)}{r_s Nu}\right]} \quad (22)$$

2.4 Energy balance at flame sheet:-

The surface energy balance at the flame sheet can be written :

$$\dot{m}_F\,\Delta hc=Q_{f-i}+Q_{f-dT} \quad (23)$$

Thus, using Fourier's Law,

$$Q_{f-i}=-\left[-4\pi l_g r_f^2\left.\frac{dT}{dr}\right|_{r_f^-}\right] \quad (24)$$

and

$$Q_{f-dT}=-4\pi l_g r_f^2\left.\frac{dT}{dr}\right|_{r_f^+} \quad (25)$$

By differentiation the temperature distribution in Eqn. (22) at the flame radius in the outer region:-

$$\left.\frac{dT}{dr}\right|_{r_f^-}=\frac{(T_f-T_{\infty})Z_T\dot{m}_F\exp\left[-\frac{Z_T\dot{m}_F}{r_f}\right]}{r_f^2\left\{\exp\left[-\frac{Z_T\dot{m}_F}{r_f}\right]-\exp\left[-\frac{Z_T\dot{m}_F(Nu-2)}{r_s Nu}\right]\right\}} \quad (26)$$

Differentiation equation for $\left(r\rightarrow r_f\right)$ at the flame radius in the inner region gives [6],

$$\left.\frac{dT}{dr}\right|_{r_f^-}=\frac{(T_s-T_f)Z_T\dot{m}_F\exp\left[-\frac{Z_T\dot{m}_F}{r_f}\right]}{r_f^2\left\{\exp\left[-\frac{Z_T\dot{m}_F}{r_s}\right]-\exp\left[-\frac{Z_T\dot{m}_F}{r_f}\right]\right\}} \quad (27)$$

Then, the energy balance at the flame yields,

$$\frac{Cp_g}{\Delta hc}\left\{\frac{(T_f-T_{\infty})\exp\left[-\frac{Z_T\dot{m}_F}{r_f}\right]}{\exp\left[-\frac{Z_T\dot{m}_F}{r_f}\right]-\exp\left[-\frac{Z_T\dot{m}_F}{r_s}\right]}\right\}-\left\{\frac{(T_f-T_{\infty})\exp\left(-\frac{Z_T\dot{m}_F}{r_f}\right)}{\exp\left[-\frac{Z_T\dot{m}_F}{r_f}\right]-\exp\left[-\frac{Z_T\dot{m}_F(Nu-2)}{r_s Nu}\right]}\right\}-1=0 \quad (28)$$

Again, five unknowns $\dot{m}_F, T_f, r_f, Y_{f,s}$, and T_s, must be evaluated assuming that the surface temperature (T_s) is equal to the boiling temperature ($T_s=T_{boil}$), This is a reasonable assumption when the droplet is burning vigorously after its initial heat-up transient and can be evaluated by the mass fraction Clausius-Clapeyron equation, by solving the Eqn. (12), (22), and (28) for the three unknowns $\dot{m}_F, T_s$, and r_f ,

(a)The evaporation rate:

The droplet mass evaporation rate in terms of the transfer number $B_{o,q}$ can be expressed by:

$$\dot{m}_F=\frac{2\pi l_g r_s Nu}{Cp_g}In\left(B_{o,q}+1\right) \quad (29)$$

Where

$$B_{o,q}=\frac{\Delta hc/u+Cp_g\left(T_{\infty}-T_s\right)}{q_{i-l}+h_{fg}}$$

(b) Flame temperature

As in pure evaporation analysis, assume the fuel is at the boiling point. The problem is greatly simplified with this assumption and by using Eqn. (12) to evaluate the flame temperature after arrogant:

$$\exp\left[-\frac{\dot{m}_F}{4\pi r D r_f}\right]=\frac{\exp\left[-\frac{\dot{m}_F(Nu-2)}{4\pi r D r_s Nu}\right]}{\frac{u+1}{u}} \quad (30)$$

If,

$$Z_F = 1/4\pi r D \quad (31)$$

Substitute Eqn. (30) and Eqn (31) into (28) yields,

$$\frac{Cp}{\Delta hc}\left\{\frac{(T_i-T_s)\exp\left[\frac{-Z_r\dot{m}_F(Nu-2)}{r_s Nu}\right]\Big/\frac{u+1}{u}}{\exp\left[\frac{-Z_r\dot{m}_F(Nu-2)}{r_s Nu}\right]\Big/\frac{u+1}{u}-\exp\left[\frac{-Z_r\dot{m}_F}{r_s}\right]}\right\}+(T_r-T_s)u=1 \quad (32)$$

Then, the flame temperature becomes:

$$T_f=\frac{uT_i\exp\left[-\frac{\dot{m}_F Cp_g(Nu-2)}{4\pi l_g r_s Nu}\right]+u^2T_s\exp\left[-\frac{\dot{m}_F Cp_g(Nu-2)}{4\pi l_g r_s Nu}\right]-u(u+1)T_s\exp\left[-\frac{\dot{m}_F Cp_g}{4\pi l_g r_s}\right]}{u\exp\left[-\frac{\dot{m}_F Cp_g(Nu-2)}{4\pi l_g r_s Nu}\right]+u^2\exp\left[-\frac{\dot{m}_F Cp_g(Nu-2)}{4\pi l_g r_s Nu}\right]-u\exp\left[-\frac{\dot{m}_F Cp_g}{4\pi l_g r_s}\right]}+\frac{\frac{\Delta h}{Cp_g}\left[\exp\left[-\frac{\dot{m}_F Cp_g(Nu-2)}{4\pi l_g r_s Nu}\right]u-\exp\left[-\frac{\dot{m}_F Cp_g}{4\pi l_g r_s}\right](u+1)\right]}{u\exp\left[-\frac{\dot{m}_F Cp_g(Nu-2)}{4\pi l_g r_s Nu}\right]+u^2\exp\left[-\frac{\dot{m}_F Cp_g(Nu-2)}{4\pi l_g r_s Nu}\right]-u\exp\left[-\frac{\dot{m}_F Cp_g}{4\pi l_g r_s}\right]} \quad (33)$$

(c) Flame stand off ratio:-

To formulate the flame stand off ratio, equation (12) is arranged to the form

$$r_f=\frac{\dot{m}_F r_s Nu}{m_F(Nu-2)+4\pi r D r_s Nu In\frac{u+1}{u}} \quad (34)$$

Then the flame stand-off ratio (ratio of the flame size to the droplet size), is given by:

$$\frac{r_f}{r_s}=\frac{\dot{m}_F Nu}{\dot{m}_F(Nu-2)+\frac{4\pi l_g}{Cp_g}r_s Nu In\frac{u+1}{u}} \quad (35)$$

(d) Droplet life time

The droplet life time is obtained using the mass balance for the classical theory which states that the rate at which the mass of the droplet decreases, is equal to the rate at which the liquid is vaporized i.e.;

$$\frac{d(m_d)}{dT}=-\dot{m}_F \quad (36)$$

where

$$m_d=\frac{\pi r_l d^3}{6} \quad (37)$$

Substituting Eqn. (29) and (37) into Eqn. (36) and differentiate, yields,

$$\frac{d(d)}{dt}=-\frac{2l_g Nu}{Cp_g r_l d}In\left[B_{o,q}+1\right] \quad (38)$$

Let

$$K=\frac{4l_g Nu}{Cp_g r_l}In\left[B_{o,q}+1\right] \quad (39)$$

or

$$d\left(d^2\right)=-Kdt \quad (40)$$

Integration of Eqn. (40) from d_o^2 to d^2 and from 0 to t given

$$d^2(t)=d_0^2-Kt \quad (41)$$

And the droplet life time will be,

$$t_d=\frac{d_0^2}{K} \quad (42)$$

(f)Damköhler number

The Damköhler number related to droplet life time is [10]:

$$Da=\frac{r_s^2}{t_d D} \quad (43)$$

3. Results and Discussion :

3.1 The Used Data

Type of Fuel: four types of fuel have been used in the calculations of the classical and extension to convective environment models which are; n-heptane, n-hexane, n-decan, and light diesel

Droplet Size: The droplet size (d) used in calculations =100μm

Environmental Conditions: The environmental conditions assumed in the calculations are:

a) Temperature: (300, 600, 1000, 1200, and 1500) K.

b) Pressure: (1) bar
c) Reynolds number at range (0.1-1800)

3.2 Extension to convective environment model and the classical model

The calculations of both the classical and extension to convective environment models for the four types of fuel under study, are based on three variables (size ratio, vaporization time, and environmental temperature), where the other parameters have been evaluated according to these three variables. Then, the comparison between the two models is held.

(a) Droplet size variation

Figures (3) and (4) show that increasing the amount of fuel vaporized from the droplet surface which in turn increases the mass vaporization rate. Higher mass vaporization has been noted for extended model due to the droplet movement that lead to a force convection case , and this in turn causes an increase in the sensible heat quantity that entering the droplet, subsequently, increasing the mass evaporation rate. Regarding the classical model, the droplet is considered as quasi-steadiness. In extended model, n-decan gives higher mass vaporization than other fuel while in classical model, light diesel has higher mass vaporization and other fuel give approximately the same behavior due to the physical properties of fuel.

(b) Burning time variation

Figures (5) and (6) show the variation of droplet size with dimensionless time of evaporation. The two models give approximately the same behavior. The curves could be divided into two parts of droplet life time, At the early stages of its lifetime the curves decrease in the droplet size with the increases of the time and this is higher than that for classical model because the droplet lifetime decreases with increase of the heat gain transfer. During the early part, a large value should be used (higher ambient temperature and higher Reynolds number), while during the later part a smaller value should be used. Therefore, at the later stages of droplet life time, the curves indicate that the behavior of n-heptane and n-hexane are the same for the classical model.

(c) Environmental temperature variation

Figures (7) and (8) for classical model, are directly related to the environmental temperature, so, any increase in the environmental temperature will lead to a noticeable increase in the flame conditions. While, in extended model, the relationship is constant due to independency on transfer number which is a function of temperature and the kind of reaction.

3.3 Comparison between the classical and extended models:-

The comparisons are carried out for characteristic parameters of n-heptane for the two models.

(a) Droplet size variation

Figure (9) shows the variation of the system Damköhler number with size for the two models. Damköhler number represents the ratio between the flow time and reaction time. So, as it is shown in the figure, Damköhler number is proportional to size, where it decreases with the decrease in size, while the variation of the system Damköhler number with size remain constant for the classical model.

(b) Vaporization time variation

Figure (10) shows that the flame temperature similarity in behavior for the two models is due to the fact that flame temperature is not affected by Nusselt number since it depends totally on the fuel properties and the environmental temperature.

(c) Environmental temperature variation

Figure (11) which show that the flame position obtained from the classical model is the most affected from temperature variation between them. And that is due to the flame position in the classical model is directly proportional to the environmental temperature since other parameters are assumed constant, while in the extended model, flame positions are approximately constant with the variation of environmental temperature due to it independent in a temperature of surrounding .

3.4 Comparison the result of extended model using different Reynolds number

Figure (12) presents that the flame stand-off ratio decreasing with increasing Reynolds number and decreasing will droplet life time due to the flame radius depending for Nusselt number.

3.5 Comparison with other works

Figure (13) presents a comparison between the extended model and work of Law [11] for $(\dot{m}_F)$ and (s) relation. The deviation between the two models is due to forced convection used in the present model while Law's model based on conduction heat transfer only.

Figure (14) reveals the comparison between present model and Law's work [11] for $(\dot{m}_F)$ and (T_∞) relation which indicates a good agreement in the behavior, especially at low temperature.

3.6 Comparison with experimental work

A comparison between present work and experimental work of Nomura [12] is presented in figure (15) for droplet size variation and life- time. A good agreement was obtained between the two works.

4. Conclusions

The following conclusions are obtained from the analysis of the obtained results:

1- Extended model has proven to be a successful model for single component calculation and has not yet been applied to droplet or other evaporation and combustion problems. The method has not been applied to transport process at all.

2- The heat up process using extended model causes the mass evaporation rate at the early stages to be much than that in the classical theory of droplet evaporation.

3- The heat transfer to the drop increases with increase Re.

4- The flame conditions (position) are not constant but, function of Re.

5- The mass evaporation rate obtained by the classical model can be corrected with a useful relation for the mass evaporation rate by the extended model for different temperature and different kind of fuel and other for different Reynold's number and different kind of fuel .

6- The flame temperature remains constant in the two models.

7-Good agreements were obtained through comparison with other work.

References

[1]. Jochen W., "Evaporation of Multicomponent Droplets", PH.D.

Thesis, Stuttgart Universidad, Aerospace Engineering, 2005.
[2]. Spalding, D. B., "Combustion and Mass Transfer", Pergamon Press, 1979.
[3]. Kamury, A. M., "Introduction to Combustion Phenomena", Gordon and Breach Science Publisher, 1975.
[4]. Sirignano, W. A., and Law, C. K., "Transient Heating and Liquid-Phase Mass Diffusion in Fuel Droplet Vaporization, Evaporation and Combustion of Fuels", Zung, editor, Adv. in Chem., Vol. 166, pp. 3, 1978.
[5] .Law, C.K., "Recent Advances in Droplet Vaporization and Combustion", Prog. Energy Combust. Sci., Vol. 8, pp. 171-201, 1982.
[6]. Turns, S. R., "An Introduction to Combustion, Concepts and Applications", Second Edition, McGraw-Hill International Editions, 2000.
[7]. Feath, G .M., "Current Status of Droplet and Liquid Combustion", Prog. Energy Combust. Sci., Vol. 3, pp. 191-224, 1977.
[8]. Ranz, W. E. and Marshall, W .R., "Evaporation from Drops", Part II, Chemical Engineering Progress, Prog. 48, pp. 173-180, 1952.
[9]. Hayes, R. E. and Kolaczkowski, S. T., "Introduction to Catalytic Combustion", Gordon and Breach Science Publishers, 1997.
[10] Dryer, F. L., "General Background for Spherically Symmetric Isolated Droplet Combustion", Princeton University, Dept. of Mechanical and Aerospace Engineering, 1997.
[11]. Law, C. K. and Law, H. K., "Theory of Quasi-Steady One-Dimensional Diffusional Combustion with Variable Properties Including Distinct Binary Diffusion Coefficients", Combustion and Flame, Vol. 29, pp. 269-275, 1977.
[12]. Tarsisius, K., "Modelling of the Heating and Evaporation of Fuel Droplets", Ph.D Thesis, School of Engineering, University of Brighton, 2007

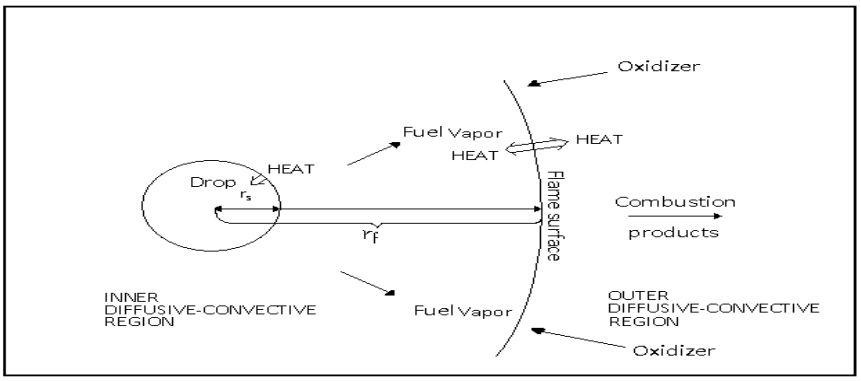

Figure (1): Vapor mole fraction and temperature profiles in gas phase through droplet evaporation

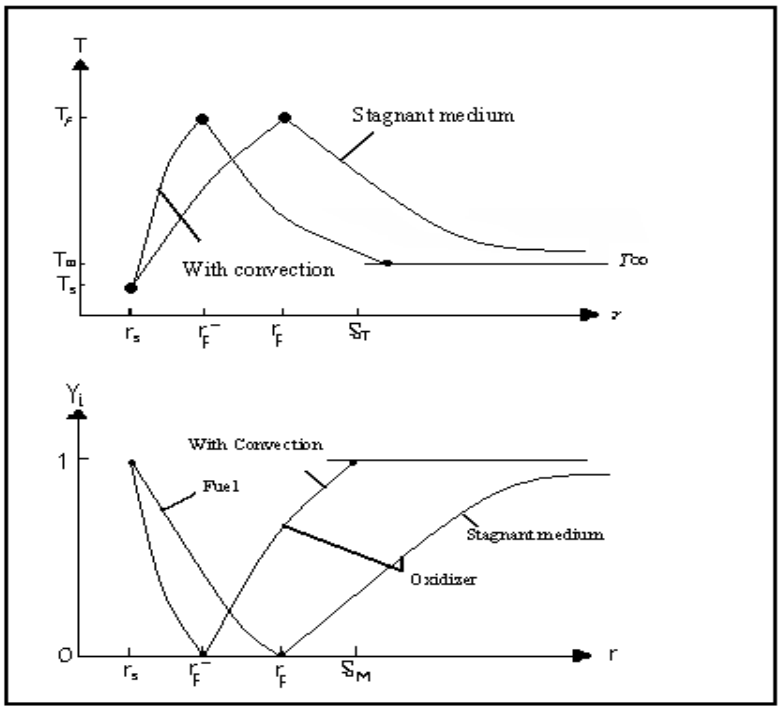

Figure (2) Comparison of temperature and species profiles with and without convection [6].

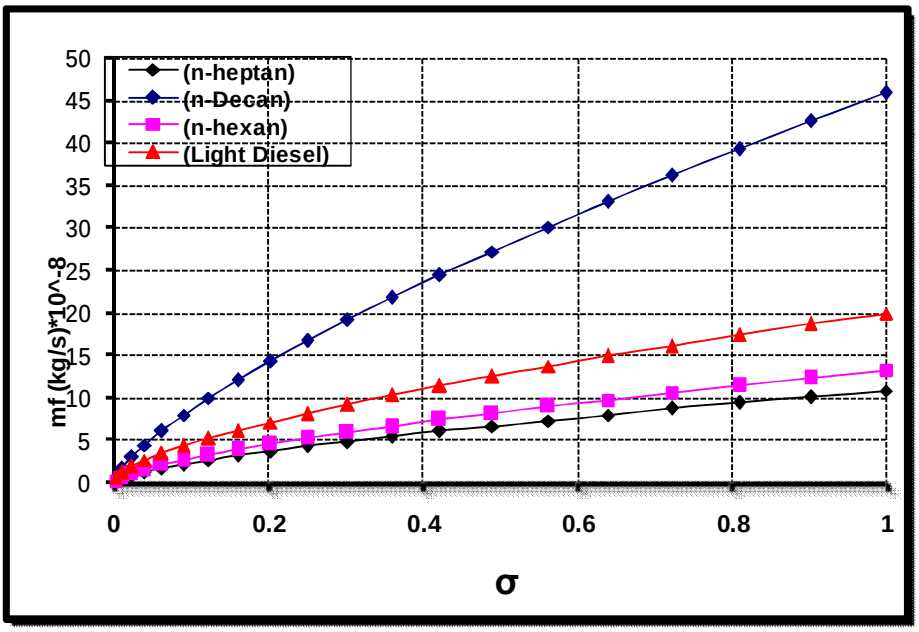

Figure (3) Variation of the mass evaporation rate with droplet size (Extended model).

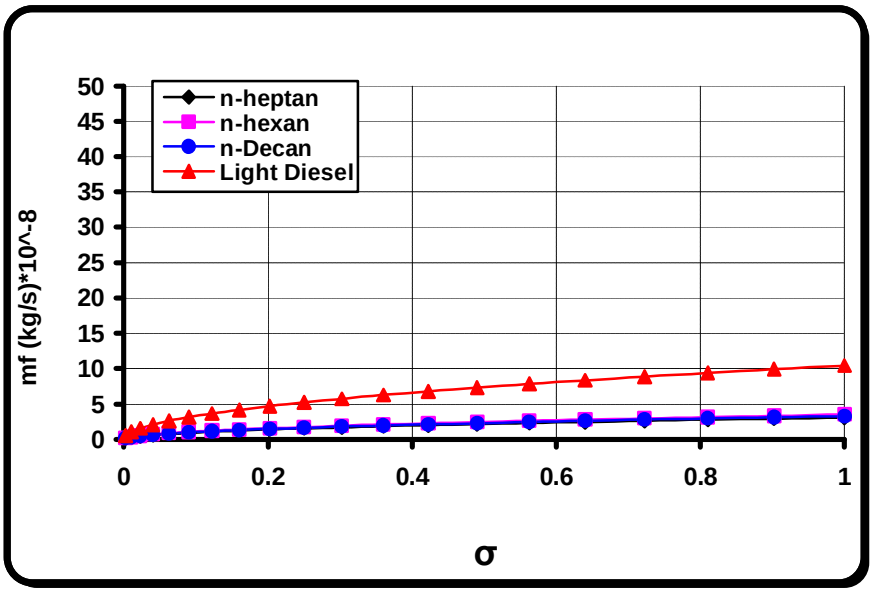

Figure (4) Variation of the mass evaporation rate with droplet (classical model) Size

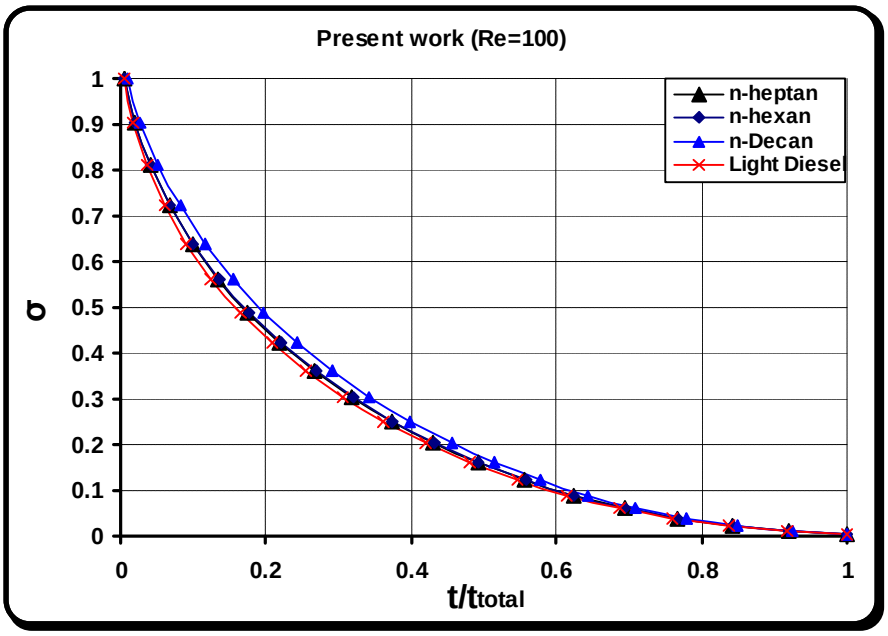

Figure (5) Size variation versus evaporation time ratio (extended model)

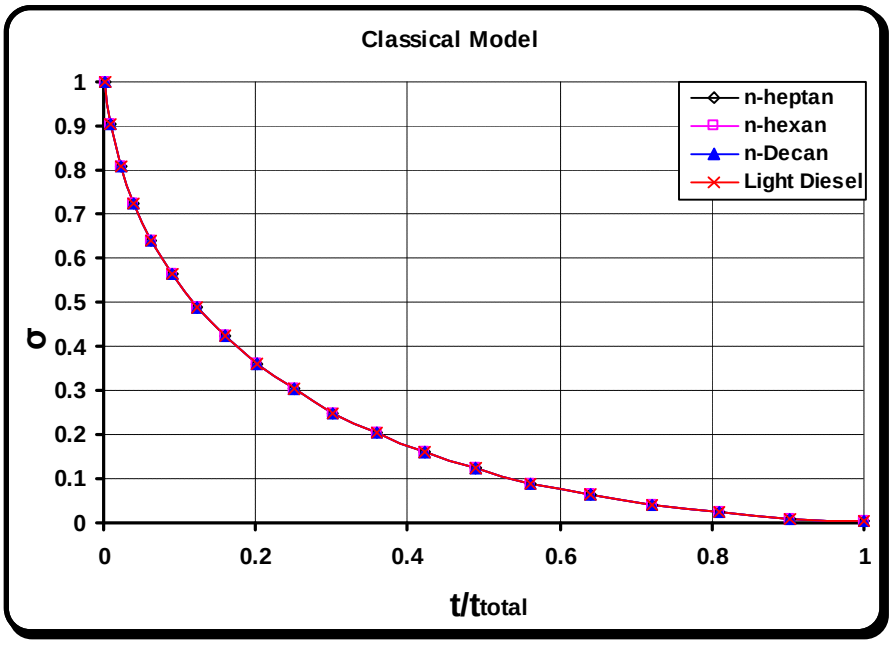

Figure (6) Size variation versus evaporation time ratio (classical model).

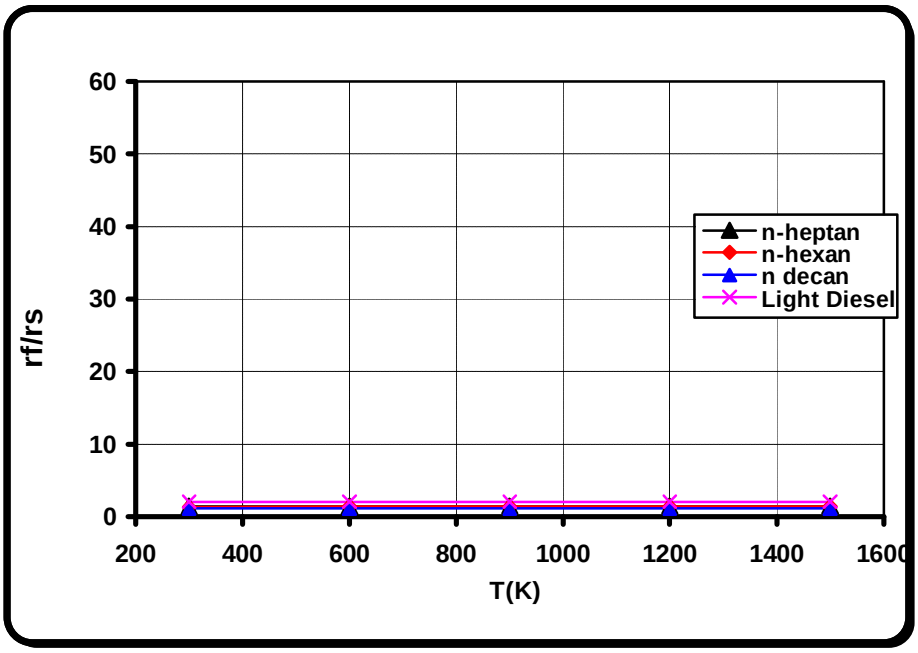

Figure (7) Variation of flame stand-off ratio with environmental temperature (extended model).

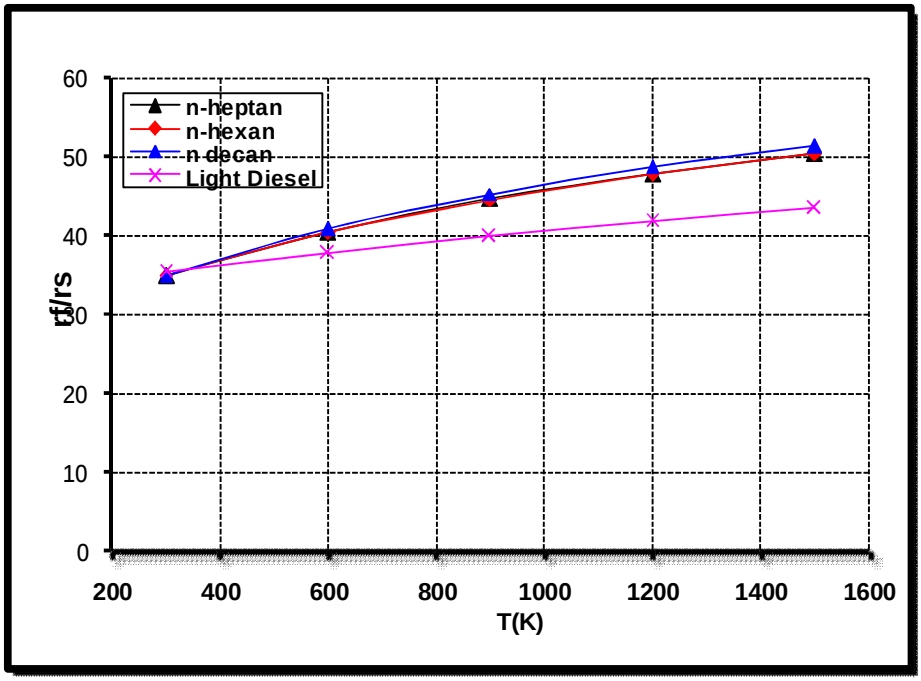

Figure (8) Variation of flame stand-off ratio with environmental temperature (classical model).

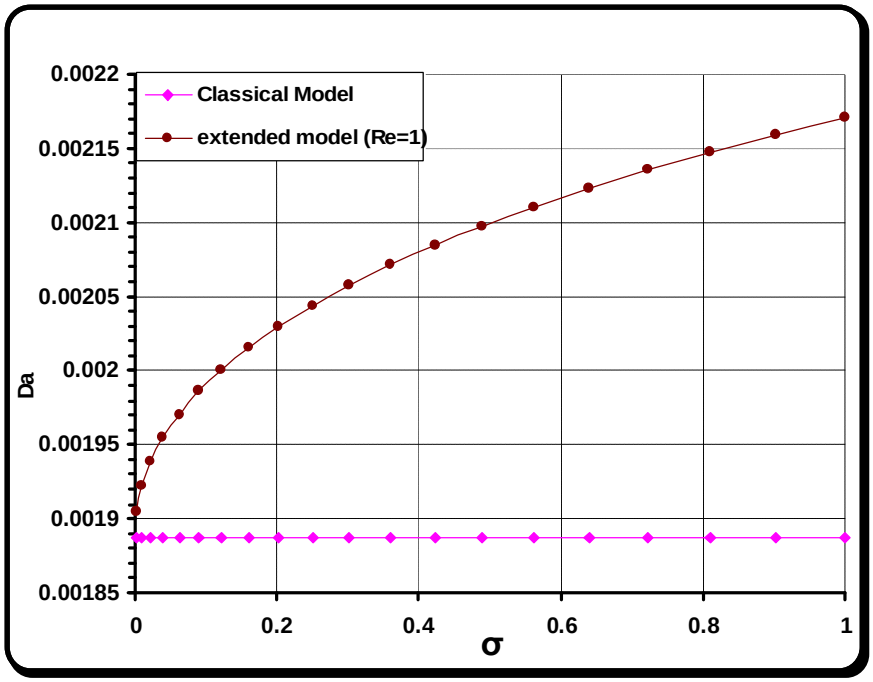

Figure (9) Variation of Damköhler number with size for (100 m m) diameter n-heptane fuel droplet under atmospheric conditions.

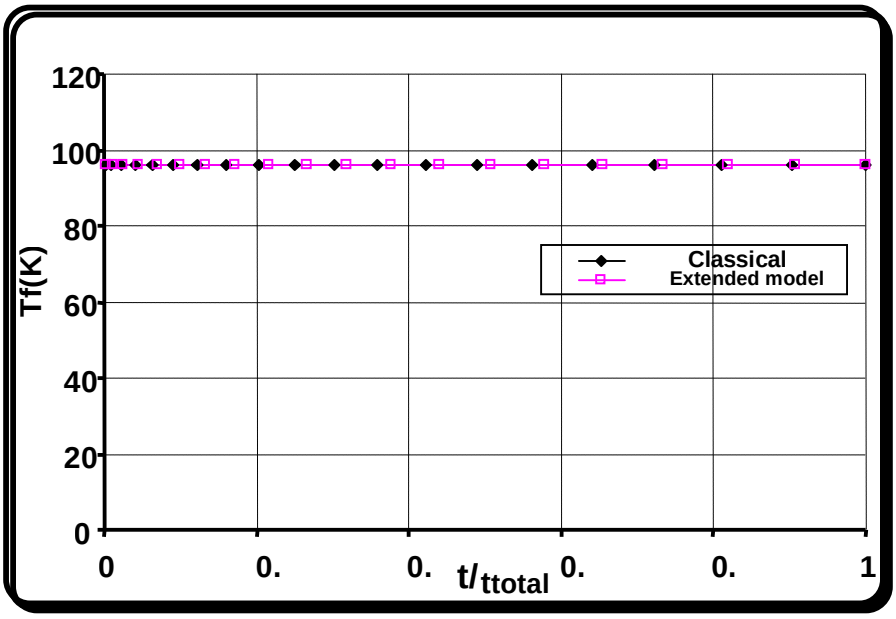

Figure (10) Variation of flame temperature with droplet evaporation time for n-heptane fuel.

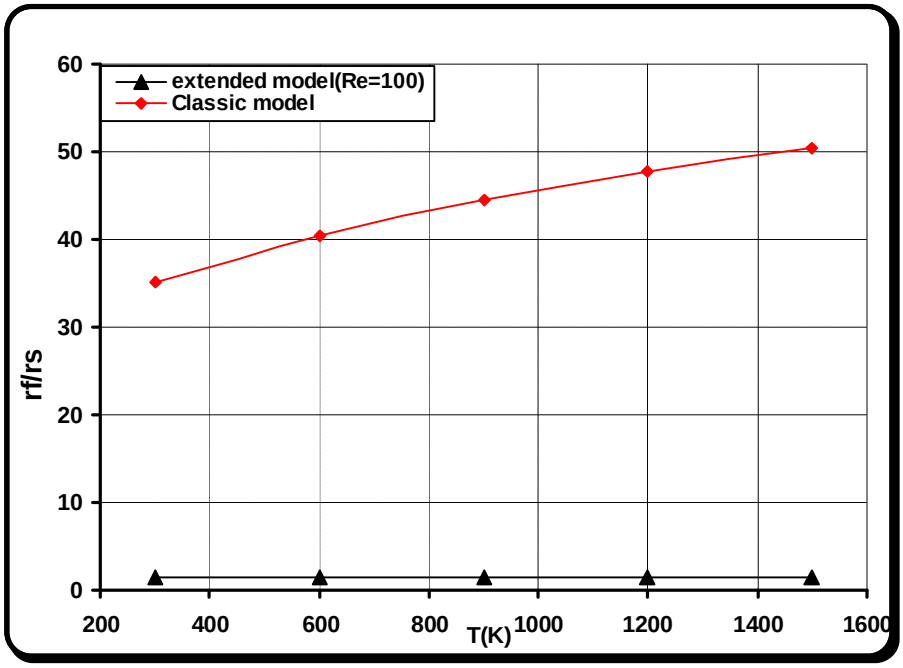

Figure (11) Variation of flame stands-off ratio with environmental Temperature for n-heptane fuel

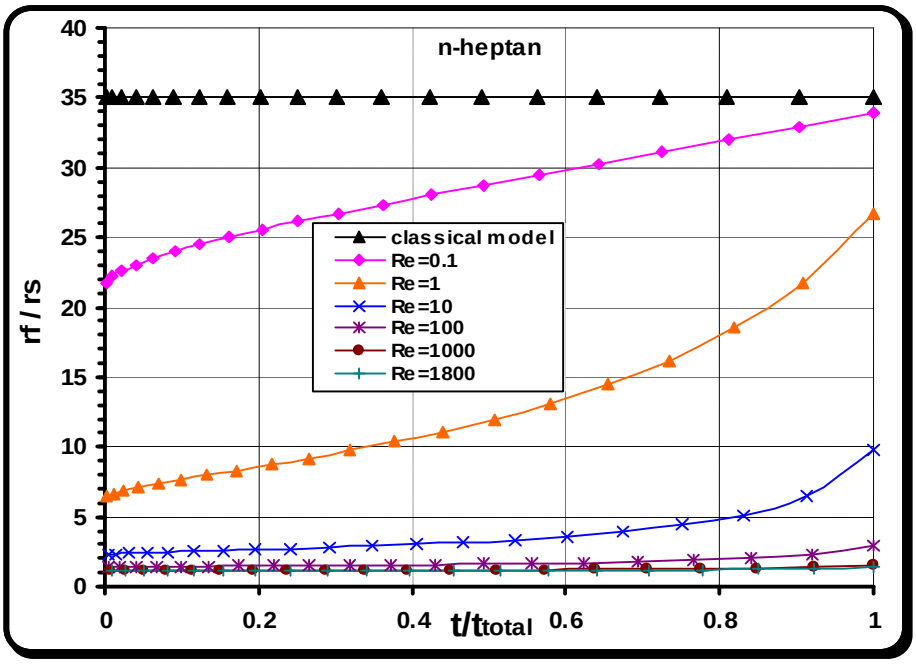

Figure (12) Flame stand-off ratio versus evaporation time ratio (Extended model) for different Reynolds number

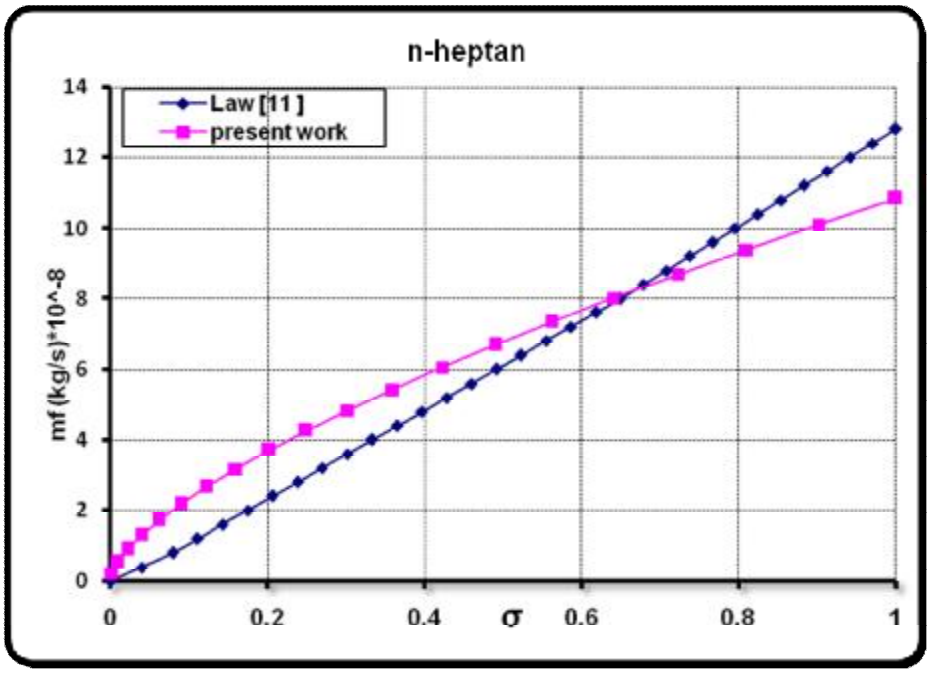

Figure (13) Comparison of the extended model and work of law [11]

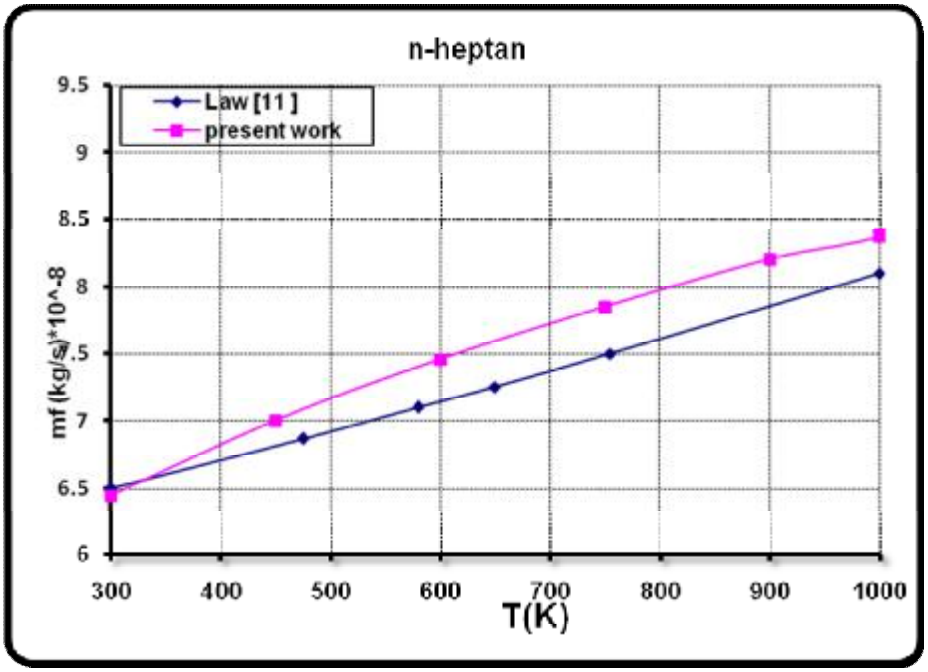

Figure (14) Comparison of the extended model and work of law [11]

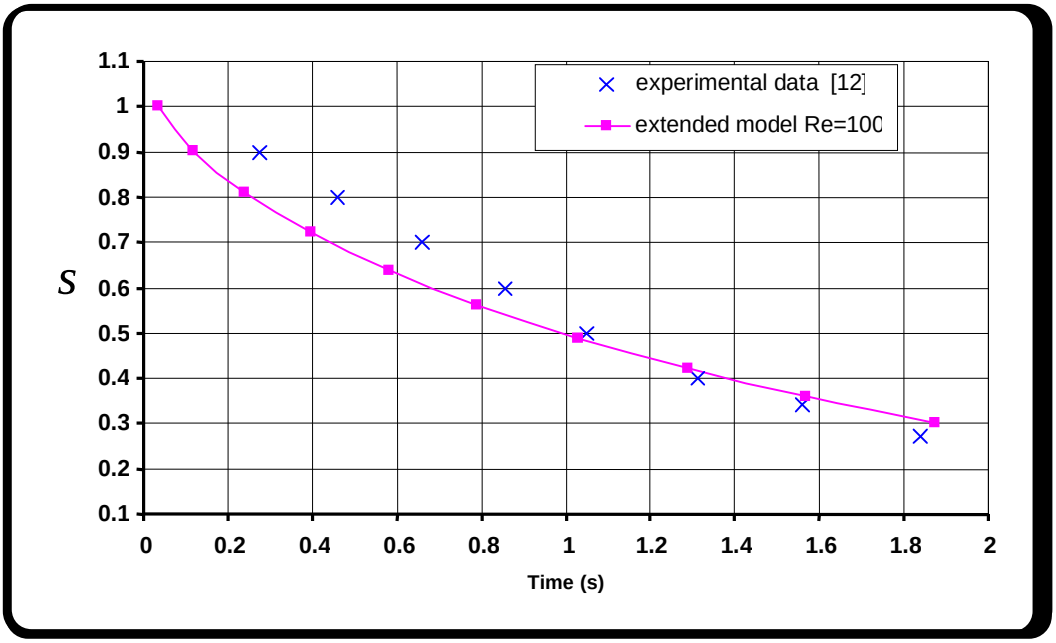

Figure (15) Size variation versus evaporation droplet lifetime (extended model) and experimental data [12].